Front. Chem. Sci. Eng. 2023, 17(11): 1801−1808
https://doi.org/10.1007/s11705-023-2325-9

RESEARCH ARTICLE

Enhancing the aromatic selectivity of cyclohexane aromatization by CO_2 coupling

Xiangxiang Ren[1,2], **Zhong-Pan Hu**[1], **Jingfeng Han** (✉)[1], **Yingxu Wei**[1], **Zhongmin Liu** (✉)[1,2,3]

1 National Engineering Research Center of Lower-Carbon Catalysis Technology, Dalian National Laboratory for Clean Energy, iChEM (Collaborative Innovation Center of Chemistry for Energy Materials), Dalian Institute of Chemical Physics, Chinese Academy of Sciences, Dalian 116023, China
2 School of Chemical Engineering, University of Chinese Academy of Sciences, Beijing 100049, China
3 State Key Laboratory of Catalysis, Dalian Institute of Chemical Physics, Chinese Academy of Sciences, Dalian 116023, China

Abstract Improving the aromatic selectivity in the alkane aromatization process is of great importance for its practical utilization but challenge to make because the high H/C ratio of alkanes would lead to a serious hydrogen transfer process and a large amount of light alkanes. Herein, CO_2 is introduced into the cyclohexane conversion process on the HZSM-5 zeolite, which can improve the aromatic selectivity. By optimizing the reaction conditions, an improved aromatic (benzene, toluene, xylene, and C_{9+}) selectivity of 48.2% can be obtained at the conditions of 2.7 MPa (CO_2), 450 °C, and 1.7 h^{-1}, which is better than that without CO_2 (aromatic selectivity = 43.2%). *In situ* transmission Fourier transform infrared spectroscopy spectra illustrate that many oxygenated chemical intermediates (e.g., carboxylic acid, anhydride, unsaturated aldehydes/ketones or ketene) would be formed during the cyclohexane conversion process in the presence of CO_2. ^{13}C isotope labeling experimental results demonstrate that CO_2 can enter into the aromatics through the formation of oxygenated chemical intermediates and thereby improve the aromatic selectivity. This study may open a green, economic, and promising way to improve the aromatic selectivity for alkane aromatization process.

Keywords aromatics, carbon dioxide, aromatization, coupling reaction, ZSM-5 zeolite

1 Introduction

Aromatics are one of the most basic raw materials in the chemical industry for the synthesis of several chemicals, such as gasoline, solvent, polyethylene terephthalate fibers, resins, and films [1]. According to the reaction temperature, the production of aromatics can be divided into low-temperature paths (methanol to aromatics [2,3], biomass conversion to aromatics [4,5], and synthesis gas conversion to aromatics [6,7], etc.) and high-temperature paths (catalytic reforming of naphtha, methane dehydroaromatization, and aromatization of short paraffin). Recently, with the development of hydraulic fracturing technologies, a large amount of shale gas (alkanes) can be extracted in this manner. Furthermore, the alkane is a kind of the main by-product of petroleum refining, coalbed gas, and steelmaking plants. Therefore, making good use of these alkanes is of great importance. In particular, cycloalkanes, as major components of naphtha, are inert and difficult to convert into high-valuable-added products. It is highly urgent to develop an efficient process to utilize cycloalkanes, in which selective conversion of alkanes to aromatics represents a kind of very promising way [8,9].

For the alkane aromatization process, two main factors should be considered, i.e., promoting the C−H dissociation and inhibiting the hydrogen transfer process. Typically, the alkane dehydrogenation process is a key factor determining the alkane aromatization process because the C−H bonds are difficult to dissociate (D_{C-H} = 414 kJ·mol^{-1}) [10,11]. Furthermore, the serious hydrogen transfer process during the alkane aromatization process would lead to many light alkanes, decreasing the aromatic selectivity [12]. Over the past several years, many methods have been exploited to improve the activity and selectivity of the alkane aromatization process. For instance, metal species (Zn [13,14], Ga [15,16], and Pt [17,18]), possessing good dehydrogenation ability, are introduced into the zeolites. Owing to the promotion of the C−H bond dissociation, the alkane aromatization

Received February 10, 2023; accepted March 14, 2023;
online June 12, 2023

E-mails: jfhan@dicp.ac.cn (Han J.), liuzm@dicp.ac.cn (Liu Z.)

process can be significantly improved. However, the hydrogen transfer process would be simultaneously promoted owing to the synergistic effect between Lewis and Brönsted acid sites, which would lead to low aromatic selectivity. Therefore, decreasing and/or eliminating the hydrogen transfer process is very necessary. Very recently, Liu and coworkers reported that the introduction of CO into the alkane aromatization process could improve the aromatic selectivity by consuming a part of hydrogen [19,20]. They found that the CO could participate in the aromatic generation by forming acyl groups and methyl-substituted cyclopentenones followed by dehydration, increasing the alkane conversion and aromatic selectivity. However, this process requires a large amount of CO (CO/*n*-hexane = 120). Therefore, developing a more effective hydrogen eliminator or inserting hydrogen-deficiency agents into the alkane aromatization process might be a good method for improving the aromatic selectivity.

CO_2, containing more oxygen than CO, might be used to eliminate a part of H_2 through the reverse water gas conversion reaction ($CO_2 + H_2 \rightarrow CO + H_2O$) and/or participate in the alkane activation and conversion by the formation of oxygenated chemical intermediates, thus promoting the formation of aromatics [21]. Furthermore, coke can be consumed by CO_2 through the reverse Boudouard reaction ($CO_2 + C \rightarrow 2CO$) to reduce the catalyst deactivation [22]. In this work, we investigated the coupling reaction process of CO_2 and cyclohexane on the HZSM-5 zeolite and realized a higher aromatic selectivity than that without CO_2. The effects of reaction temperature, weight hourly space velocity (WHSV) of cycloalkane, and system pressure on the coupling reaction process were studied. The participation of CO_2 in the coupling reaction process was analyzed by an *in situ* transmission Fourier Transform infrared spectroscopy (FTIR), and the possible reaction mechanism was proposed. Furthermore, ^{13}C isotope tracer experiments were performed to reveal the role of CO_2 during the coupling reaction process including the consumption of excess hydrogen and the participation in the aromatization.

2 Experimental

2.1 Catalyst and characterization

All HZSM-5 zeolites were purchased from Nankai University. The zeolites were characterized by X-ray fluorescence analysis, X-ray powder diffraction (XRD), ammonia temperature-programmed desorption (NH_3-TPD), solid-state magic-angle spinning nuclear magnetic resonance spectra of ^{27}Al (^{27}Al MAS NMR) and pyridine-adsorbed FTIR (py-IR). All results were shown in the Electronic Supplementary Material (ESM) section.

2.2 Catalytic tests

The HZSM-5 zeolite powder was pressed under 35 MPa pressure and granulated. The 40–60 mesh zeolite particles were selected for experiments. The detailed part of the experiment is shown in the ESM section.

3 Results and discussion

3.1 Cyclohexane-CO_2 aromatization on HZSM-5 zeolite

The XRD pattern (Fig. S1, cf. ESM) and NH_3-TPD result (Fig. S2, cf. ESM) suggest the HZSM-5 (SiO_2/Al_2O_3 = 38) zeolite possesses a well-defined MFI structure and an acid amount of 1.00 $mmol_{NH_3} \cdot g^{-1}$. The ^{27}Al MAS NMR spectrum (Fig. S3, cf. ESM) shows two peaks at 56.5 and 0 ppm, corresponding to the framework and non-framework Al, respectively. This indicates that the HZSM-5 zeolite used is mainly composed of tetra-coordinated framework Al. Besides, the Brönsted and Lewis acidity of HZSM-5 zeolite is analyzed by FTIR spectra of pyridine adsorption/desorption (Fig. S4, cf. ESM). Typically, pyridine molecules adsorbed to the Lewis acid sites give rise to the FTIR bands at 1450, 1490 and 1610 cm^{-1}, while pyridine molecules adsorbed on the Brönsted acid sites give rise to FTIR bands at 1490, 1540 and 1640 cm^{-1} [23,24]. These FTIR bands can be observed over the HZSM-5 zeolite after pyridine adsorption and evacuation at 100 °C, indicating the presence of both Brönsted and Lewis acid sites. Moreover, the bands at 1640 and 1540 cm^{-1} are much stronger than those at 1610 and 1450 cm^{-1}, indicating the presence of a large amount of Brönsted acid sites and only a slight of Lewis acid sites which is in good accordance with the ^{27}Al MAS NMR results (Fig. S3). To make clear the role of CO_2 during the cyclohexane aromatization process, the system pressure, reaction temperature, CO_2 pressure, WHSV, and the SiO_2/Al_2O_3 ratio of HZSM-5 zeolite are all investigated (Figs. 1, S5 and Tables S1–S6, cf. ESM).

First, the influence of the system pressure on the coupling reaction process is investigated (Fig. 1(a)). At the atmospheric pressure, the cyclohexane conversion (X_{CYH}), aromatic selectivity ($S_{aromatics}$), and CO_2 conversion (X_{CO_2}) are 75.8%, 38.9%, and 0.85% respectively. After increasing the system pressure to 3 MPa, the X_{CYH}, $S_{aromatics}$, and X_{CO_2} can be improved to around 100%, 48.2%, and 4.67%, respectively, suggesting the high system pressure is good for the coupling reaction process.

The influence of CO_2 pressure on the coupling reaction process of cyclohexane is presented (Fig. 1(b)). At low CO_2 pressure of 1.0 MPa, no obvious changes in the aromatic selectivity can be observed during the cyclohexane aromatization process. When the CO_2 pressure is increased from 0 to 2.0 MPa, the aromatic selectivity can

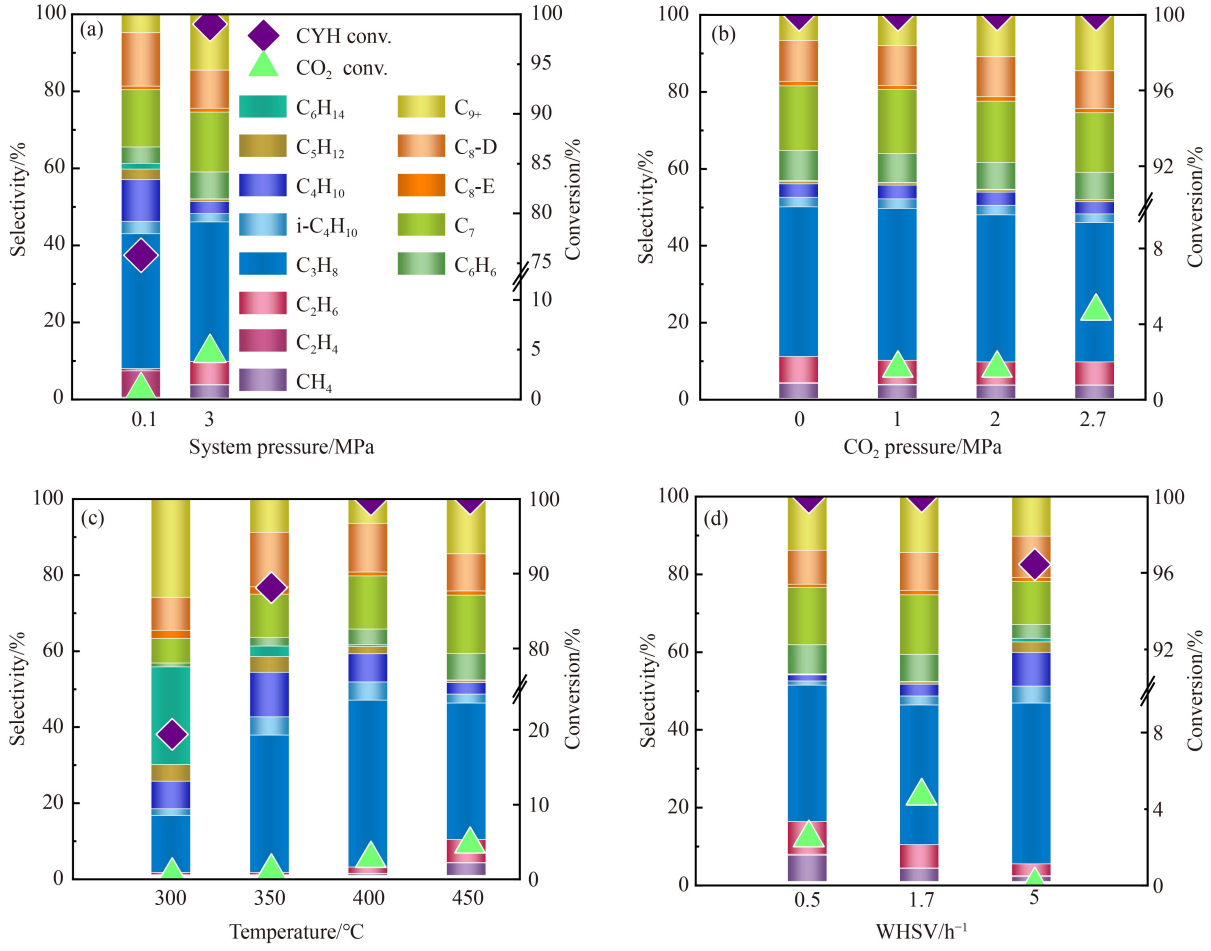

Fig. 1 (a) The CO_2 conversion, cyclohexane conversion and product selectivity at the system pressures of 0.1 and 3 MPa; (b) the CO_2 conversion, cyclohexane conversion and product selectivity at the CO_2 pressures of 0, 1, 2 and 2.7 MPa; (c) the CO_2 conversion, cyclohexane conversion and product selectivity at the reaction temperatures of 300, 350, 400 and 450 °C; (d) the CO_2 conversion, cyclohexane conversion and product selectivity at the WHSV of cyclohexane of 0.5, 1.7 and 5 h^{-1}. Reaction conditions: TOS = 1.0 h, (CO_2 + N_2)/cyclohexane = 13.

be improved from 43.2% to 45.5%. With further increasing the CO_2 pressure to 2.7 MPa, the aromatic selectivity can be increased to 48.2%. These results suggest the addition of CO_2 can improve the reaction of cyclohexane aromatization. In addition, the CO_2 conversion increases from 1.67% to 4.67% with increasing the CO_2 pressure from 1 to 2.7 MPa, illustrating more CO_2 molecules are involved in the reaction at a high CO_2 pressure.

The effect of reaction temperature on the coupling reaction process of cyclohexane and CO_2 is investigated (Fig. 1(c)). With increasing the reaction temperature from 300 to 450 °C, the cyclohexane conversion increases rapidly from 19.4% to 99.9%, and the CO_2 conversion of increases from 0.57% to 4.67%. This suggests the cyclohexane aromatization is a thermodynamically controlled reaction that needs a high reaction temperature. Furthermore, the effect of SiO_2/Al_2O_3 ratios of HZSM-5 zeolite on the coupling reaction process of cyclohexane and CO_2 is investigated (Fig. S5). With decreasing the SiO_2/Al_2O_3 ratio of HZSM-5 zeolite from 1500 to 38, the cyclohexane conversion increases from 40.2% to 99.9%, and the CO_2 conversion increases from 0.44% to 4.67%, indicating the high acidity of zeolite is good for the coupling reaction process of cyclohexane and CO_2 to aromatics.

Figure 1(d) shows the cyclohexane conversion and the different product selectivities at different WHSV values. At a low WHSV of 0.5 h^{-1}, cyclohexane molecules can be fully converted with an aromatic selectivity of 46.2%. With increasing the WHSV to 1.7 h^{-1}, ~100% cyclohexane conversion with an aromatic selectivity of 48.2% can be achieved. Further increasing the WHSV to 5.0 h^{-1}, the cyclohexane conversion is reduced to 96.4%, and the aromatic selectivity decreases to 36.9%, probably because the residence time is too low to realize the cyclohexane conversion at high WHSV. Noticeably, the CO_2 conversion is a little different to cyclohexane conversion at different WHSV. At a low WHSV of 0.5 h^{-1}, the CO_2 conversion is 2.49%. When the WHSV increases to 1.7 h^{-1}, the CO_2 conversion is increased to 4.67%.

However, further increasing the WHSV to 5.0 h^{-1}, the CO_2 conversion is dramatically reduced to 0.03%.

3.2 *In situ* transmission FTIR study

To identify the role of CO_2 and better understand the coupling reaction process, *in situ* transmission FTIR studies, retained species studies and isotope experiments were performed on HZSM-5 zeolite (Fig. 2). First, the coupling reaction process is studied by *in situ* transmission FTIR (Fig. 2(a)). The band at 1757 cm^{-1} can be attributed to the C=O stretching vibration of lactone [25], indicating the lactone intermediates are formed at the initial stage by CO_2 insertion. C−O−H out-of-plane bending vibration in the 953 cm^{-1} bands is attributed to the carboxylic acid [26], suggesting the lactone is decomposed with the reaction time. The bands at 1840 and 1787 cm^{-1} are attributed to the C=O antisymmetric stretching vibration of acid anhydride and the C=O symmetric stretching vibration of acid anhydride, respectively [27,28]. These signals indicate that the carboxylic acid species will convert to acid anhydride. Furthermore, the band at 1690 cm^{-1} can be observed, corresponding to the C=O stretching vibration of unsaturated aldehydes/ketones [29]. After a certain time, two obvious bands at 903 and 854 cm^{-1} can be observed, which can be attributed to the out-of-plane bending vibration of aromatic ring C−H [30], suggesting the formation of aromatics.

In situ transmission FTIR study on the coupling reaction process of cyclohexane and $^{13}CO_2$ is carried out to identify the intermediates. With the introduction of $^{13}CO_2$, the peak positions of lactones, carboxylic acids, anhydrides, unsaturated aldehydes/ketones, aromatics, etc. are redshifted by 30 to 70 cm^{-1} (Fig. 2(b)). The C=O stretching vibration of lactone shifts from 1757 to 1698 cm^{-1} [31]. The C−O−H out-of-plane bending vibration of carboxylic acid shifts from 953 to 892 cm^{-1} [32]. The C=O symmetric stretching and antisymmetric stretching vibrations of acid anhydride move from 1840 to 1770 cm^{-1} and 1787 to 1730 cm^{-1}, respectively [33]. The C=O stretching vibration of unsaturated aldehyde/ketone shifts from 1690 to 1652 cm^{-1} [34,35]. The C−H out-of-plane bending vibration of the aromatic ring moves from 903 to 827 cm^{-1} and from 854 to 804 cm^{-1}, respectively [36,37]. These results confirm the formation of oxygenated chemical intermediates during the coupling

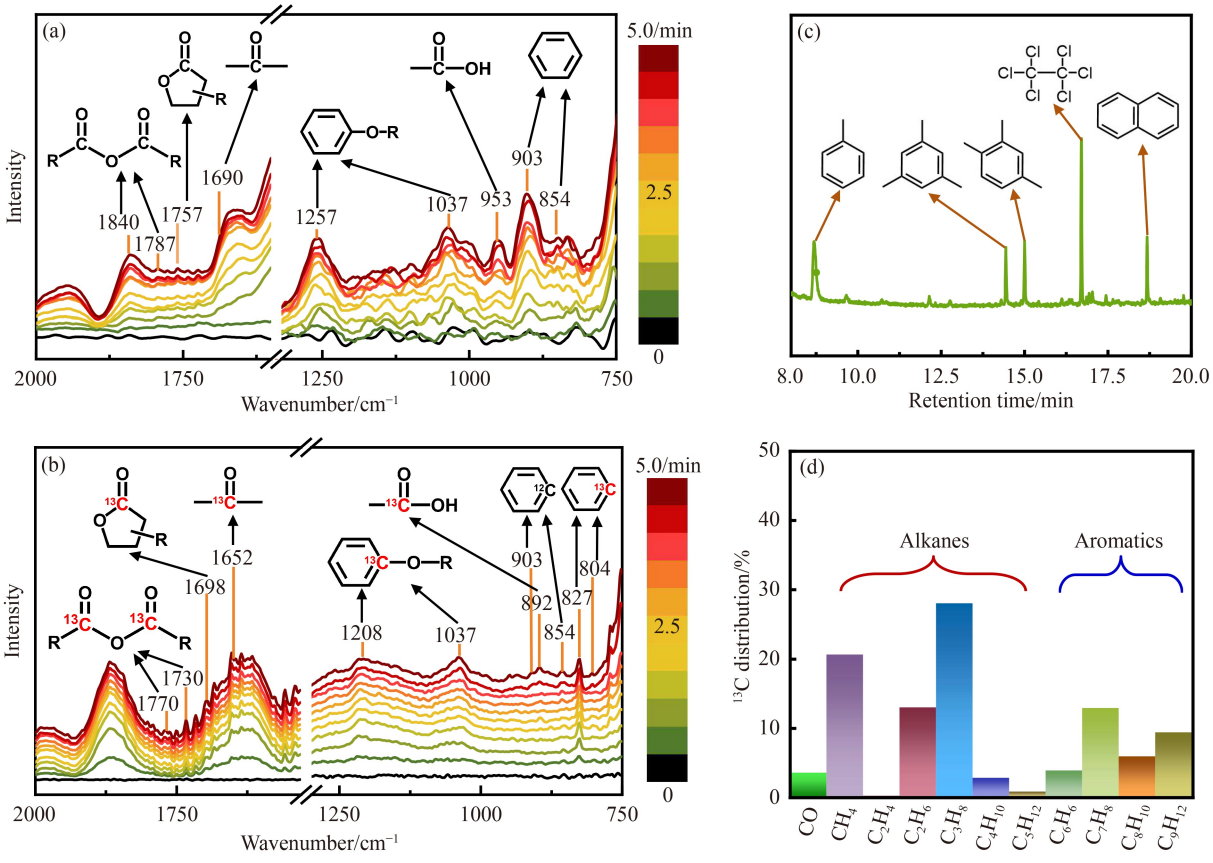

Fig. 2 (a) *In situ* transmission FTIR spectra of the coupling reaction process of cyclohexane and $^{12}CO_2$ over the HZSM-5 zeolite; (b) *in situ* transmission FTIR spectra of the coupling reaction process of cyclohexane and $^{13}CO_2$ over the HZSM-5 zeolite; (c) GC-MS spectrum of the retained species on the spent HZSM-5 zeolite after the coupling reaction process (retention times up to 20 min); (d) ^{13}C distribution in the effluent products during the coupling reaction of cyclohexane with $^{13}CO_2$ over the HZSM-5 zeolite. Reaction conditions: t = 450 °C, SiO_2/Al_2O_3 = 38, P_{system} = 0.5 MPa, P_{CO_2} = 0.43 MPa, (CO_2 + N_2)/cyclohexane = 13.

reaction process of cyclohexane and CO_2, suggesting the CO_2 molecules participate in the aromatic generation during the aromatization process.

In addition, the spent HZSM-5 zeolite (t = 450 °C, SiO_2/Al_2O_3 = 38, P_{system} = 0.5 MPa, P_{CO_2} = 0.43 MPa) is dissolved into 40% HF solution, extracted with dichloromethane (containing 10 ppm hexachloroethane), and then analyzed by GC-MS (Fig. 2(c)). The carbon deposition products contain a high proportion of aromatics. However, no oxygenated chemical intermediates can be detected over the spent HZSM-5 zeolite, which is not consistent with the FTIR results, probably because the oxygenated chemical intermediates are highly active and convert into aromatics.

To confirm the role of CO_2, $^{13}CO_2$ is used instead of $^{12}CO_2$ and the products were detected by GC-MS (Fig. 2(d)). It is shown that CO_2 is involved in three main processes. ~4% CO_2 is converted to CO (Fig. S6, cf. ESM), suggesting a part of CO_2 participates in the elimination of hydrogen through the reverse water gas reaction. At the same time, 65% CO_2 is converted into light alkanes, indicating most CO_2 participates in the hydrogen transfer process during the coupling reaction process. 31% CO_2 is converted into aromatics, suggesting CO_2 can enter into the final aromatics by intercalation of the C−O bond to form alkoxy groups. However, no oxygenated chemical intermediates can be observed in Fig. 2(c), which may be due to the fact that the oxygenated chemical intermediates are highly active at the reaction temperature of 450 °C.

3.3 Discussion and mechanism

Based on the above catalytic results and characterizations, the system pressure, CO_2 pressure, reaction temperature, and WHSV have great influences on the coupling reaction process of cyclohexane and CO_2. Typically, increasing the system pressure (from atmospheric pressure to 3.0 MPa) can improve the cyclohexane conversion and the aromatic selectivity (Fig. 1(a)). It is reported that the high reaction pressure can promote the dehydrogenation process and depress the diffusion of products, thus promoting the aromatization process [38]. The *in situ* transmission FTIR (Figs. 2(a) and 2(b)) and the CO_2 pressure experimental results (Fig. 1(b)) reveal that CO_2 can eliminate a part of H_2 by the formation of oxygenated chemical intermediates such as lactones [21]. Then, the lactones can be further converted into carboxylic acids, anhydrides, unsaturated aldehydes/ketones or ketene. This result is in good consistent with our previous work about alkanes-CO coupling to aromatics [19,20]. The different temperature experiments reveal that the cyclohexane aromatization process in the presence of CO_2 is a thermodynamically controlled reaction that requires high reaction temperature (Fig. 1(c)). Particularly, the high reaction temperature is good for the C−H dissociation and C−C bond coupling [39].

Besides, the WHSV can affect the cyclohexane aromatization process by influencing the contact time between cyclohexane and HZSM-5 zeolite (Fig. 1(d)). When the contact time is low (WHSV = 5.0 h^{-1}), cyclohexane molecules cannot be activated, resulting in low conversion (X_{CYH} = 96.4%) and aromatic selectivity ($S_{aromatics}$ = 37.0%) [40,41]. However, too long contact time (WHSV = 0.5 h^{-1}) would result in serious side reactions (such as heavy aromatization and/or coke formation), which would lead to low aromatic selectivity ($S_{aromatics}$ = 46.2%). The residual species on the spent HZSM-5 zeolite are analyzed, showing no oxygen-containing species (Fig. 2(c)). However, the *in situ* transmission FTIR results show many oxygenated chemical intermediates. Also, isotope experiments reveal that the CO_2 molecules are incorporated into the CO (4%), alkanes (65%) and aromatics (31%) during the cyclohexane aromatization process (Fig. 2(d)), suggesting CO_2 cannot only transform into CO through eliminating a part of H_2 and can also enter into the aromatics via forming oxygenated chemical intermediates.

Combining with the *in situ* transmission FTIR characterizations and isotopic-labeled experimental results, a possible reaction path for the cycloalkane-CO_2 coupling reaction process is proposed (Fig. 3). In the absence of CO_2, cyclohexane is activated at the Brönsted acid centers, and then olefins are formed through cracking and oligomerization. Subsequently, olefins will be transformed into aromatics by hydrogen transfer, cyclization and dehydrogenation processes. At the same time, low-carbon alkanes such as methane, ethane and propane are produced, which is one of the key factors resulting in low aromatic selectivity [42]. In the presence of CO_2, cyclohexane is first activated at the Brönsted acid centers and then reacts with CO_2 to form lactone. After that, carboxylic acid, anhydride and other oxygenated chemical intermediates would be formed through the ring-opening process. Then, the oxygenated chemical intermediates will be dehydrated, resulting in unsaturated aldehydes/ketones or ketene [43–45]. On one hand, the unsaturated aldehydes/ketones or ketene would be cyclized to cyclic ketones and transform into dienes and/or aromatics through dehydration, hydrogen transfer and rearrangement processes. On the other hand, unsaturated aldehydes/ketones or ketene would be dehydrated to dienes and then dehydrogenated to aromatics. Meanwhile, CO_2 participates in the elimination of hydrogen in the coupling reaction process through the reverse water gas reaction ($CO_2 + H_2 \rightarrow CO + H_2O$).

4 Conclusions

Herein, CO_2 is exploited as an efficient assistant to

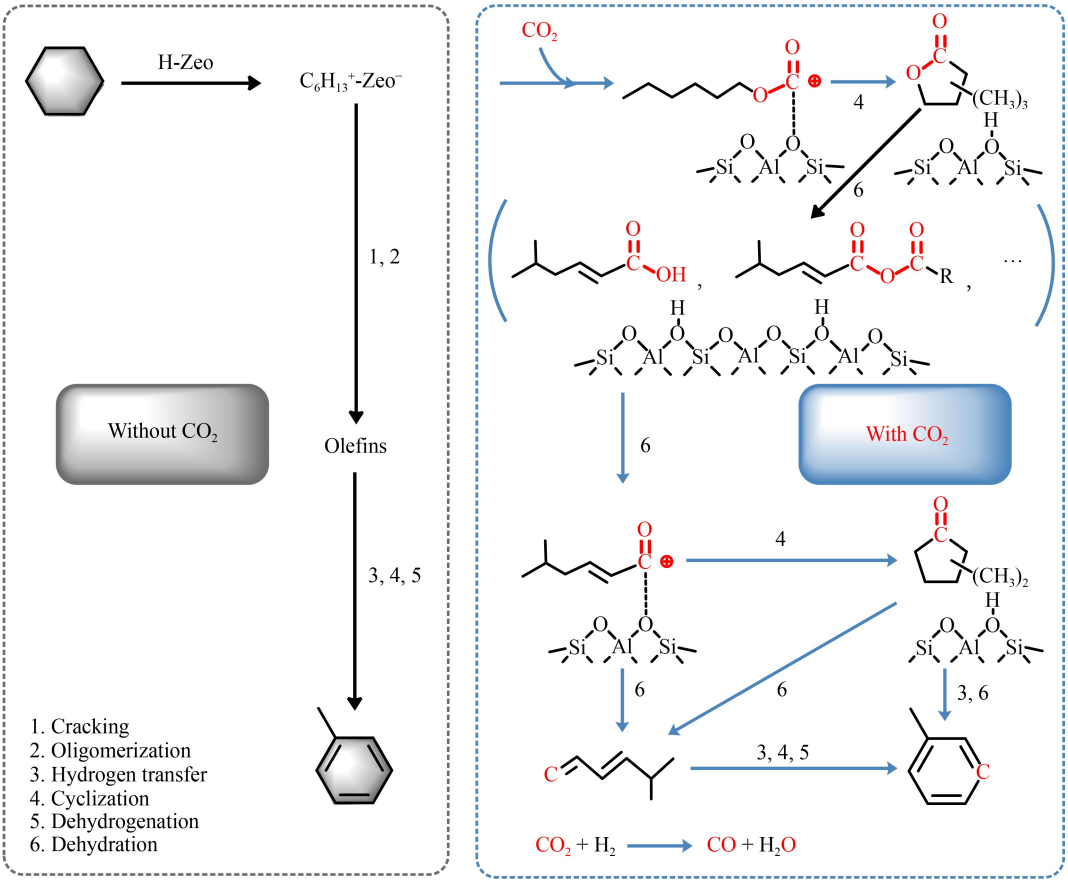

Fig. 3 Proposed mechanism of the aromatic formation for the coupling reaction process of CO_2 and cyclohexane over HZSM-5 zeolite.

improve the aromatic selectivity during the cyclohexane aromatization process. The reaction conditions including system pressure, CO_2 pressure, reaction temperature, and WHSV are systematically investigated. It is found that the aromatic selectivity can be improved at a reaction condition of suitable reaction temperature (⩾ 450 °C), high system pressure and CO_2 pressure (> 1 MPa), and appropriate WHSV (< 5.0 h^{-1}). The optimized reaction results (X_{CYH} = 100%, X_{CO_2} = 4.7%, $S_{aromatics}$ = 48.2%) can be obtained at the temperature of 450 °C, the CO_2 pressure of 2.7 MPa, and the WHSV of 1.7 h^{-1}. The role of CO_2 in the coupling reaction process is revealed by *in situ* transmission FTIR spectra and ^{13}C-labeled experiments. CO_2 can participate in the aromatization via the formation of lactone, carboxylic acid, anhydride, and other oxygenated chemical intermediates. Subsequently, these oxygenated chemical intermediates containing carbonyl and ester groups could be converted into aromatic precursors such as ketenes, alkenes/cycloalkenes, or dienes/cyclodienes, and finally transform into aromatics. The $^{13}CO_2$ isotope tracing experiment shows that 65% of the carbon atoms of CO_2 can enter into alkanes, 31% into aromatics, and 4% into CO. This study represents an efficient and environment-friendly strategy for the improvement of aromatic selectivity from the alkane aromatization process on zeolite-based materials.

Conflicts of interest There are no conflicts to declare.

Acknowledgements This work was supported by the National Key Research and Development Program of China (Grant No. 2022YFE0116000), the National Natural Science Foundation of China (Grant Nos. 22202193, 21991092, 21991090, 22172166 and 22288101), the China Postdoctoral Science Foundation (Grant No. 2019M661147), the Excellent Postdoctoral Support Program of Dalian Institute of Chemical Physics, CAS, the Excellent Research Assistant Funding Project of CAS, the Youth Innovation Promotion Association CAS (Grant No. 2021182), the Innovation Research Foundation of Dalian Institute of Chemical Physics, Chinese Academy of Sciences (Grant No. DICP I202217)

Electronic Supplementary Material Supplementary material is available in the online version of this article at https://doi.org/10.1007/s11705-023-2325-9 and is accessible for authorized users.

References

1. Tomás R A F, Bordado J C M, Gomes J F P. *p*-Xylene oxidation to terephthalic acid: a literature review oriented toward process optimization and development. Chemical Reviews, 2013, 113(10): 7421–7469
2. Zhang G Q, Bai T, Chen T F, Fan W T, Zhang X. Conversion of methanol to light aromatics on Zn-modified nano-HZSM-5 zeolite catalysts. Industrial & Engineering Chemistry Research, 2014, 53(39): 14932–14940

3. Chen Z, Ni Y, Zhi Y, Wen F, Zhou Z, Wei Y, Zhu W, Liu Z. Coupling of methanol and carbon monoxide over H-ZSM-5 to form aromatics. Angewandte Chemie International Edition, 2018, 57(38): 12549–12553
4. Ye L, Song Q, Lo B T W, Zheng J, Kong D, Murray C A, Tang C C, Tsang S C E. Decarboxylation of lactones over Zn/ZSM-5: elucidation of the structure of the active site and molecular interactions. Angewandte Chemie International Edition, 2017, 56(36): 10711–10716
5. Carlson T R, Vispute T P, Huber G W. Green gasoline by catalytic fast pyrolysis of solid biomass derived compounds. ChemSusChem, 2008, 1(5): 397–400
6. Gilani S Z A, Lu L, Arslan M T, Ali B, Wang Q, Wei F. Two-way desorption coupling to enhance the conversion of syngas into aromatics by MnO/H-ZSM-5. Catalysis Science & Technology, 2020, 10(10): 3366–3375
7. Nawaz M A, Li M, Saif M, Song G, Wang Z, Liu D. Harnessing the synergistic interplay of Fischer–Tropsch synthesis (Fe–Co) bimetallic oxides in Na-FeMnCo/HZSM-5 composite catalyst for syngas conversion to aromatic hydrocarbons. ChemCatChem, 2021, 13(8): 1966–1980
8. Zhang Y, Wu S, Xu X, Jiang H. Ethane aromatization and evolution of carbon deposits over nanosized and microsized Zn/ZSM-5 catalysts. Catalysis Science & Technology, 2020, 10(3): 835–843
9. Yuan J, Zhou S, Peng T, Wang G, Ou X M. Petroleum substitution, greenhouse gas emissions reduction and environmental benefits from the development of natural gas vehicles in china. Petroleum Science, 2018, 15(3): 644–656
10. Bernstein H J. Bond energies in hydrocarbons. Transactions of the Faraday Society, 1962, 58: 2285–2306
11. Hu Z P, Qin G, Han J, Zhang W, Wang N, Zheng Y, Jiang Q, Ji T, Yuan Z Y, Xiao J, Wei Y, Liu Z. Atomic insight into the local structure and microenvironment of isolated Co-motifs in MFI zeolite frameworks for propane dehydrogenation. Journal of the American Chemical Society, 2022, 144(27): 12127–12137
12. Hu Z P, Yang D, Wang Z, Yuan Z Y. State-of-the-art catalysts for direct dehydrogenation of propane to propylene. Chinese Journal of Catalysis, 2019, 40(9): 1233–1254
13. Rodrigues V d O. Faro Júnior A C. On catalyst activation and reaction mechanisms in propane aromatization on Ga/HZSM5 catalysts. Applied Catalysis A: General, 2012, 435–436: 68–77
14. Liu D, Cao L, Zhang G, Zhao L, Gao J, Xu C. Catalytic conversion of light alkanes to aromatics by metal-containing HZSM-5 zeolite catalysts—a review. Fuel Processing Technology, 2021, 216: 106770
15. Rane N, Kersbulck M, van Santen R A, Hensen E J M. Cracking of *n*-heptane over Brønsted acid sites and lewis acid Ga sites in ZSM-5 zeolite. Microporous and Mesoporous Materials, 2008, 110(2): 279–291
16. Dooley K M, Chang C, Price G L. Effects of pretreatments on state of gallium and aromatization activity of gallium/ZSM-5 catalysts. Applied Catalysis A: General, 1992, 84(1): 17–30
17. Yu C, Xu H, Ge Q, Li W. Properties of the metallic phase of zinc-doped platinum catalysts for propane dehydrogenation. Journal of Molecular Catalysis A: Chemical, 2007, 266(1): 80–87
18. Zhang Y, Zhou Y, Tang M, Liu X, Duan Y. Effect of la calcination temperature on catalytic performance of PtSnNaLa/ZSM-5 catalyst for propane dehydrogenation. Chemical Engineering Journal, 2012, 181–182: 530–537
19. Wei C, Yu Q, Li J, Liu Z. Coupling conversion of *n*-hexane and CO over an HZSM-5 zeolite: tuning the H/C balance and achieving high aromatic selectivity. ACS Catalysis, 2020, 10(7): 4171–4180
20. Wei C, Li J, Yang K, Yu Q, Zeng S, Liu Z. Aromatization mechanism of coupling reaction of light alkanes with CO over acidic zeolites: cyclopentenones as key intermediates. Chem Catalysis, 2021, 1(6): 1273–1290
21. Niu X, Nie X, Yang C, Chen J G. CO_2-assisted propane aromatization over phosphorus-modified Ga/ZSM-5 catalysts. Catalysis Science & Technology, 2020, 10(6): 1881–1888
22. Gomez E, Nie X, Lee J H, Xie Z, Chen J G. Tandem reactions of CO_2 reduction and ethane aromatization. Journal of the American Chemical Society, 2019, 141(44): 17771–17782
23. Buzzoni R, Bordiga S, Ricchiardi G, Lamberti C, Zecchina A, Bellussi G. Interaction of pyridine with acidic (H-ZSM5, H-β, H-MORD zeolites) and superacidic (H-Nafion membrane) systems: an IR investigation. Langmuir, 1996, 12(4): 930–940
24. Li P, Liu G, Wu H, Liu Y, Jiang J G, Wu P. Postsynthesis and selective oxidation properties of nanosized Sn-beta zeolite. Journal of Physical Chemistry C, 2011, 115(9): 3663–3670
25. Zhou J, Lu G, Wu S. A new approach for the synthesis of α-methylene-γ-butyrolactones from α-bromomethyl acrylic acids (or esters). Synthetic Communications, 1992, 22(4): 481–487
26. Gao X, Leng C, Zeng G, Fu D, Zhang Y, Liu Y. Ozone initiated heterogeneous oxidation of unsaturated carboxylic acids by ATR-FTIR spectroscopy. Spectrochimica Acta Part A: Molecular and Biomolecular Spectroscopy, 2019, 214: 177–183
27. Gu X, Yang C Q. FTIR spectroscopy study of the formation of cyclic anhydride intermediates of polycarboxylic acids catalyzed by sodium hypophosphite. Textile Research Journal, 2000, 70(1): 64–70
28. Frederick B G, Ashton M R, Richardson N V, Jones T S. Orientation and bonding of benzoic acid, phthalic anhydride and pyromellitic dianhydride on Cu(110). Surface Science, 1993, 292(1): 33–46
29. Lievens C, Mourant D, He M, Gunawan R, Li X, Li C Z. An FT-IR spectroscopic study of carbonyl functionalities in bio-oils. Fuel, 2011, 90(11): 3417–3423
30. Margoshes M, Fassel V A. The infrared spectra of aromatic compounds: I. The out-of-plane C–H bending vibrations in the region 625–900 cm^{-1}. Spectrochimica Acta, 1955, 7(1): 14–24
31. Noguchi T, Sugiura M. Analysis of flash-induced FTIR difference spectra of the S-state cycle in the photosynthetic water-oxidizing complex by uniform ^{15}N and ^{13}C isotope labeling. Biochemistry, 2003, 42(20): 6035–6042
32. Hage W, Hallbrucker A, Mayer E. Metastable intermediates from glassy solutions. Part 3. FTIR spectra of α-carbonic acid and its ^{2}H and ^{13}C isotopic forms, isolated from methanolic solution. Journal of the Chemical Society, Faraday Transactions, 1996, 92(17): 3183–3195
33. Goodall J J, Booth V K, Ashcroft A E, Wharton C W. Hydrogen-

bonding in 2-aminobenzoyl-α-chymotrypsin formed by acylation of the enzyme with isatoic anhydride: IR and mass spectroscopic studies. ChemBioChem, 2002, 3(1): 68–75

34. Zeko T, Hannigan S F, Jacisin T, Guberman Pfeffer M J, Falcone E R, Guildford M J, Szabo C, Cole K E, Placido J, Daly E, Kubasik M A. FT-IR spectroscopy and density functional theory calculations of ^{13}C isotopologues of the helical peptide Z-Aib6-OtBu. Journal of Physical Chemistry B, 2014, 118(1): 58–68
35. Sivasankar N, Frei H. Direct observation of kinetically competent surface intermediates upon ethylene hydroformylation over Rh/Al_2O_3 under reaction conditions by time-resolved fourier transform infrared spectroscopy. Journal of Physical Chemistry C, 2011, 115(15): 7545–7553
36. Painter P C, Koenig J L. Liquid phase vibrational spectra of ^{13}C-isotopes of benzene. Spectrochimica Acta Part A: Molecular Spectroscopy, 1977, 33(11): 1003–1018
37. Clarkson J, Ewen Smith W. A DFT analysis of the vibrational spectra of nitrobenzene. Journal of Molecular Structure, 2003, 655(3): 413–422
38. Le Noble W J, Brower K R, Brower C, Chang S. Pressure effects on the rates of aromatization of hexamethyl (dewar benzene) and dewar benzene. Volume as a factor in crowded molecules. Journal of the American Chemical Society, 1982, 104(11): 3150–3152
39. Lombardo E A, Hall W K. The mechanism of isobutane cracking over amorphous and crystalline aluminosilicates. Journal of Catalysis, 1988, 112(2): 565–578
40. You H. Influence of aromatization reaction conditions in the presence of HZSM-5 catalyst. Petroleum Science and Technology, 2006, 24(6): 707–716
41. Krishnamurthy G, Bhan A, Delgass W N. Identity and chemical function of gallium species inferred from microkinetic modeling studies of propane aromatization over Ga/HZSM-5 catalysts. Journal of Catalysis, 2010, 271(2): 370–385
42. Ma Z, Hou X, Chen B, Zhao L, Yuan E, Cui T. Analysis of *n*-hexane, 1-hexene, cyclohexane and cyclohexene catalytic cracking over HZSM-5 zeolites: effects of molecular structure. Reaction Chemistry & Engineering, 2022, 7(8): 1762–1778
43. Chen W, Li G, Yi X, Day S J, Tarach K A, Liu Z, Liu S B, Edman Tsang S C, Góra Marek K, Zheng A. Molecular understanding of the catalytic consequence of ketene intermediates under confinement. Journal of the American Chemical Society, 2021, 143(37): 15440–15452
44. Jiao F, Pan X, Gong K, Chen Y, Li G, Bao X. Shape-selective zeolites promote ethylene formation from syngas via a ketene intermediate. Angewandte Chemie International Edition, 2018, 57(17): 4692–4696
45. Jiao F, Li J, Pan X, Xiao J, Li H, Ma H, Wei M, Pan Y, Zhou Z, Li M, Miao S, Li J, Zhu Y, Xiao D, He T, Yang J, Qi F, Fu Q, Bao X. Selective conversion of syngas to light olefins. Science, 2016, 351(6277): 1065–1068